Heat Transfer Research, 2010, Vol. 41, No. 3

Experiments and Simulations in Transient Conjugated Conduction–Convection–Radiation

CAROLINA P. NAVEIRA-COTTA[a*], MOHAMMED LACHI[b],

MOURAD REBAY[b], and RENATO M. COTTA[a]

[a]Mechanical Engineering Department — COPPE & POLI — UFRJ,
Universidade Federal do Rio de Janeiro,
Cx. Postal 68503 — Rio de Janeiro,
RJ — Brasil — 21945-970

[b]Laboratoire GRESPI — Thermomécanique, Faculté des Sciences
PB1039, 51687 Reims, France

Experimental results and hybrid numerical-analytical simulations are critically compared for transient laminar forced convection over flat plates of non-negligible thickness, subjected to an applied wall heat flux at the fluid–solid wall interface. A conjugated conduction–convection–radiation problem is first formulated and then simplified through the employment of the Coupled Integral Equations Approach (CIEA) to reformulate the heat conduction problem on the plate by averaging the related energy equation in the transversal direction. A partial differential formulation for the transversally averaged wall temperature is obtained, and the boundary condition for the fluid in the heat balance at the solid–fluid interface is then rewritten. The coupled partial differential equations within the thermal boundary layer are handled by the Generalized Integral Transform Technique (GITT) under its partial transformation mode, combined with the method of lines implemented in the *Mathematica* 7.0 routine *NDSolve*. For the experiments, an apparatus was employed involving an air blower and flash lamps that heat a vertical PVC plate of 33 cm in length and 12 mm in thickness, while the temperature at the surface exposed to the cooling air is measured by infrared thermography. Thermocouple measurements are also utilized to provide estimates of heat losses at the back surface of the plate. The transient evolution of the measured surface temperatures along the plate length are then critically com-

*Address all correspondence to C. P. Naviera-Cotta E-mail: cpncotta@hotmail.com

ISSN1064-2285

pared against the simulation results in order to verify the proposed model.

* * *

Key words: forced convection, conjugated problem, infrared thermography, integral transforms

1. INTRODUCTION

The pioneering works of Perelman [1] and Luikov et al. [2] on conjugated convection–conduction heat transfer problems have been challenging thermal sciences researchers along the last few decades. In engineering practice, most conjugated problems are handled in an iterative manner, by successively solving the convection and conduction problems, eventually incorporating a radiation boundary condition, or just by fully neglecting the coupling between the phenomena when accuracy is not at a premium. As one of the classical heat transfer problems, which frequently appears in thermal engineering applications, it remains open in terms of exact analytical treatment. Nevertheless, hybrid numerical-analytical approaches are particularly well suited in providing solutions to conjugated problems, which may lead to both accuracy improvement with respect to the simplified engineering approaches and reduced computational involvement in comparison to purely numerical methods [3–7]. One such hybrid approach that has been previously employed in the solution of conjugated problems is known as the Generalized Integral Transform Technique (GITT), belonging to a class of methods that combine eigenfunction expansions with the numerical solution of transformed differential systems [8–12]. On the other hand, the analysis of transient forced convection problems has renewed the interest on interpretation of conjugation effects, in light of the marked influence of both thermal capacitance and resistance of the solid walls on the fluid thermal behavior [13–16]. A number of mixed experimental and theoretical works have also reported attempts to quantify and covalidate the convective behavior under such transient conjugated conditions [17–19]. Also quite recently, a hybrid solution again based on the Generalized Integral Transform Technique has been proposed to transient conjugated conduction–external convection problems [20, 21], which provided important physical interpretation of the transient heat flux partition between the solid and the fluid for an imposed heat flux at the solid–fluid interface.

Transient laminar forced convection over flat plates of non-negligible thickness, subjected to an applied wall heat flux at the fluid–solid interface, is thus analyzed here. The work is aimed at verifying both the heat transfer modeling and the hybrid numerical-analytical solution methodology recently developed [20, 21] with the aid of an experimental investigation with infrared thermography [18, 19]. A conjugated conduction–convection–radiation model is constructed through the employment of the

Coupled Integral Equations Approach (CIEA) [9, 22] so as to reformulate the heat conduction problem on the plate, by averaging the related energy equation in the transversal direction. As a result, a partial differential formulation for the transversally averaged wall temperature is obtained, rewriting the boundary condition for the fluid in the heat balance at the solid–fluid interface. From the available theoretical velocity distributions, the solution method is then proposed for the coupled partial differential equations within the thermal boundary layer, based on the Generalized Integral Transform Technique (GITT) [8]. The GITT is utilized under its partial transformation mode, combined with the method of lines implemented in the *Mathematica* computational system [23]. For the experimental results, an apparatus was employed involving an air blower to cool, and flash lamps to heat, a vertical PVC plate of 33 cm in length and 12 mm in thickness, while the exposed surface temperature is measured by infrared thermography. Fluxmeter and thermocouple measurements are also utilized to covalidate the infrared camera measurements and to provide estimates of heat losses. The experimental configuration provides insulating boundaries in all surfaces of the slab that are not being heated by the flash, but heat losses by natural convection and radiation may still occur in all non-illuminated faces. The transient evolution of the measured surface temperatures along the plate length is critically compared against the simulation results, and the model is then analyzed to illustrate the major effects that require refinement for a closer agreement with the experimental findings.

2. PROBLEM FORMULATION AND SOLUTION METHODOLOGY

The problem analyzed here is a more general version of that proposed by Naveira et al. [21], so as to adequate the mathematical formulation to the experimental conditions, as will be discussed in what follows. It involves laminar incompressible flow of a Newtonian fluid over a flat plate, with steady-state flow but transient conjugated heat transfer due to a possibly time- and space-variable non-contact heat flux, $\phi(x^*, t)$, applied at the solid–fluid interface. The fluid flows with a free stream velocity u_∞, which arrives at the plate front edge at a temperature $T_\infty(t)$, which may vary along the process. The wall is considered to participate in the heat transfer problem, with thickness e, and length L, exchanging heat by both convection to the fluid and radiation to the surroundings. Heat losses are also allowed at all the other surfaces not directly heated by the applied front face heat flux. The boundary layer equations are assumed to be valid for the flow and heat transfer problem within the fluid. Thus, the energy equations for the fluid and for the solid are given by:

$$\frac{\partial T_f(x^*,y^*,t)}{\partial t} + u\frac{\partial T_f(x^*,y^*,t)}{\partial x^*} + v\frac{\partial T_f(x^*,y^*,t)}{\partial y^*} = \alpha_f \frac{\partial^2 T_f(x^*,y^*,t)}{\partial y^{*2}}, \tag{1a}$$

$$0 < y^* < \delta_t^*(x^*,t)\ ,\ 0 < x^* < L\ ,\ t > 0,$$

$$\frac{\partial T_s(x^*,y^*,t)}{\partial t}=\alpha_s\left(\frac{\partial^2 T_s(x^*,y^*,t)}{\partial x^{*2}}+\frac{\partial^2 T_s(x^*,y^*,t)}{\partial y^{*2}}\right),\ -e<y^*<0\ ,\ 0<x^*<L\ ,\ t>0 \quad (1b)$$

with the initial, boundary, and interface conditions

$$f_T(x^*,y^*,0)=T_\infty(0)\quad ,\ 0<y^*<\infty\ ,\ 0<x^*<L, \quad (1c)$$

$$T_s(x^*,y^*,0)=T_\infty(0)\quad ,\ -e<y^*<0\ ,\ 0<x^*<L, \quad (1d)$$

$$T_f(x^*,\delta_t^*,t)=T_\infty(t)\quad ,\qquad 0<x^*<L\ ,\ t>0, \quad (1e)$$

$$T_f(x^*,0,t)=T_s(x^*,0,t)\quad ,\ 0<x^*<L\ ,\ t>0, \quad (1f)$$

$$-k_f\left.\frac{\partial T_f}{\partial y^*}\right|_{y^*=0}=-k_s\left.\frac{\partial T_s}{\partial y^*}\right|_{y^*=0}+\varphi(x^*,t)-\varepsilon(x^*)\sigma\left(T_s^4(x^*,0,t)-T_\infty^4(t)\right),\ 0<x^*<L\ ,\ t>0, \quad (1g)$$

$$-k_s\left.\frac{\partial T_s}{\partial y^*}\right|_{y^*=-e}=h_{eff}(x^*,t)\left(T_\infty(t)-T_s\right)\ ,\quad 0<x^*<L\ ,\ t>0, \quad (1h)$$

$$T_f(0,y^*,t)=T_\infty(t)\quad ,\qquad 0<y^*<\infty\ ,\ t>0, \quad (1i)$$

$$-k_s\left.\frac{\partial T_s}{\partial x^*}\right|_{x^*=0}=h_0(t)\left(T_\infty(t)-T_s\right),\quad -e<y^*<0\ ,\ t>0, \quad (1j)$$

$$-k_s\left.\frac{\partial T_s}{\partial x^*}\right|_{x^*=L}=h_L(t)\left(T_\infty(t)-T_s\right)\ ,\quad -e<y^*<0\ ,\ t>0. \quad (1k)$$

As compared to the analysis in [21], the proposed problem, Eqs. (1), incorporates the possibility of heat losses also through all the solid boundaries that are not in direct contact with the flowing stream, through the specification of appropriate heat transfer coefficients at the boundary conditions, Eqs. (1h), (1j), and (1k), besides the time varying free stream temperature and space and time variable prescribed interface heat flux. Most important, the present model allows for the conjugation with radiative heat transfer at the fluid–solid interface, with a space variable emissivity, and permits that a variable effective heat transfer coefficient be specified at the back surface of the plate, that may or may not be insulated.

The formulation may now be simplified through the proposition of a lumped formulation for the wall, integrating its temperature field along the transversal direction, y^*. Instead of employing the Classical Lumped System Analysis, which essentially assumes the wall temperature field to be uniform in the transversal direction, an im-

proved model is proposed obtained via the Coupled Integral Equations approach (C.I.E.A.) [9, 22] based on Hermite-type approximations for integrals. We consider just the two approximations, $H_{0,0}$ and $H_{1,1}$, which correspond, respectively, to the well-known trapezoidal and corrected trapezoidal integration rules, given by:

$$H_{0,0} \rightarrow \int_a^b f(y)\,dy \cong \frac{(b-a)}{2}\big(f(a)+f(b)\big), \tag{2a}$$

$$H_{1,1} \rightarrow \int_a^b f(y)\,dy \cong \frac{(b-a)}{2}\big(f(a)+f(b)\big)+\frac{(b-a)^2}{12}\big(f'(a)+f'(b)\big). \tag{2b}$$

The transversally averaged wall temperature is then approximated by taking the $H_{1,1}$ approximation, the corrected trapezoidal rule. In addition, the transversally averaged heat flux at the solid wall is approximated by the $H_{0,0}$ approximation, the trapezoidal rule. This $H_{1,1}/H_{0,0}$ combined solution does not change the nature of the problem in comparison with the classical lumped formulation, but only modifies the equation coefficients. Also, it has been shown to be significantly more accurate than the classical lumped system analysis in the applicable range of the governing parameters [9]. The transversally averaged wall temperature, $T_{\mathrm{av}}(x^*, t)$, is thus approximated as:

$$T_{\mathrm{av}}(x^*,t) \equiv \frac{1}{e}\int_{-e}^{0} T_{\mathrm{s}}(x^*,y^*,t)\,dy^*$$

$$\approx \frac{1}{2}\big[T_{\mathrm{s}}(x^*,0,t)+T_{\mathrm{s}}(x^*,-e,t)\big]+\frac{e}{12}\left[\left.\frac{\partial T_{\mathrm{s}}}{\partial y^*}\right|_{y^*=-e}-\left.\frac{\partial T_{\mathrm{s}}}{\partial y^*}\right|_{y^*=0}\right], \tag{3a}$$

The average heat flux is approximated as:

$$\frac{k_{\mathrm{s}}}{e}\int_{-e}^{0}\frac{\partial T_{\mathrm{s}}(x^*,y^*,t)}{\partial y^*}\,dy^* \equiv \frac{k_{\mathrm{s}}}{e}\big[T_{\mathrm{s}}(x^*,0,t)-T_{\mathrm{s}}(x^*,-e,t)\big]$$

$$\approx \frac{k_{\mathrm{s}}}{e}\,\frac{e}{2}\left[\left.\frac{\partial T_{\mathrm{s}}}{\partial y^*}\right|_{y^*=-e}+\left.\frac{\partial T_{\mathrm{s}}}{\partial y^*}\right|_{y^*=0}\right]. \tag{3b}$$

An expression for the temperature at the plate back face, $y^* = -e$, is thus obtained from Eq. (3a):

$$T_{\mathrm{s}}(x^*,-e,t) = \frac{e k_{\mathrm{s}}\left.\dfrac{\partial T_{\mathrm{s}}}{\partial y^*}\right|_{y^*=0} + 12\,k_{\mathrm{s}}T_{\mathrm{av}}(x^*,t) - 6k_{\mathrm{s}}T_{\mathrm{s}}(x^*,0,t) + e\,h_{\mathrm{eff}}(x^*,t)\,T_{\infty}(t)}{e\,h_{\mathrm{eff}}(x^*,t)+6k_{\mathrm{s}}}. \tag{4a}$$

This expression is substituted into the average heat flux expression, Eq. (3b), providing:

$$\left.\frac{\partial T_s}{\partial y^*}\right|_{y^*=0}$$

$$=\frac{2\left[6k_s\left(T_s(x^*,0,t)-T_{av}(x^*,t)\right)+e\,h_{eff}(x^*,t)\left(2T_s(x^*,0,t)+T_\infty(t)-3T_{av}(x^*,t)\right)\right]}{e\left(e\,h_{eff}(x^*,t)+4k_s\right)} \quad (4b)$$

For no heat losses at the back face of the plate, i.e., $h_{eff} = 0$, as shown in [21], the above relation is reduced to:

$$\left.\frac{\partial T_s}{\partial y^*}\right|_{y^*=0}=\frac{3}{e}\left[T_f(x^*,0,t)-T_{av}(x^*,t)\right]. \quad (4c)$$

The interface condition, Eq. (1g), is then written as:

$$-k_f\left.\frac{\partial T_f}{\partial y^*}\right|_{y^*=0}=\varphi(x^*,t)-\varepsilon\sigma(T_f^4(x^*,0,t)-T_\infty^4(t))$$

$$-k_s\frac{2\left[6k_s\left(T_f(x^*,0,t)-T_{av}(x^*,t)\right)+e\,h_{eff}(x^*,t)\left(2T_f(x^*,0,t)+T_\infty(t)-3T_{av}(x^*,t)\right)\right]}{e\left(e\,h_{eff}(x^*,t)+4k_s\right)} \quad (4d)$$

The energy equation for the solid is now reformulated by taking the average in the transversal direction, operating it with $\frac{1}{e}\int_{-e}^{0} dy^*$, to yield:

$$\left.\frac{\partial T_{av}(x^*,t)}{\partial t}\right|_{y^*=0}=\alpha_s\frac{\partial^2 T_{av}(x^*,t)}{\partial x^{*2}}+\frac{\alpha_s}{e}\int_{-e}^{0}\frac{\partial^2 T_s(x^*,y^*,t)}{\partial y^{*2}}dy^*$$

$$=\alpha_s\frac{\partial^2 T_{av}(x^*,t)}{\partial x^{*2}}+\frac{\alpha_s}{e}\left[\left.\frac{\partial T_s(x^*,y^*,t)}{\partial y^*}\right|_{y^*=0}-\left.\frac{\partial T_s(x^*,y^*,t)}{\partial y^*}\right|_{y^*=-e}\right]. \quad (5)$$

We can then eliminate the derivatives at $y^* = 0$ and at $y^* = -e$ by applying the boundary condition, Eq. (1h), and the developed expressions (4a) and (4b), to find:

$$\frac{\partial T_{av}(x^*,t)}{\partial t}=\alpha_s\frac{\partial^2 T_{av}(x^*,t)}{\partial x^{*2}}$$

$$+\frac{12\alpha_s k_s\left(T_f(x^*,0,t)-T_{av}(x^*,t)\right)-e\alpha_s\left[6h_{eff}(x^*,t)\left(-2T_{av}(x^*,t)+T_f(x^*,0,t)+T_\infty(t)\right)\right]}{e^2\left(eh_{eff}(x^*,t)+4k_s\right)}. \quad (6a)$$

Again, for no heat losses at the back face of the plate, i.e., $h_{\text{eff}} = 0$, the above re-formulated energy equation simplifies to:

$$\frac{\partial T_{\text{av}}(x^*,t)}{\partial t} = \alpha_{\text{s}} \frac{\partial^2 T_{\text{av}}(x^*,t)}{\partial x^{*2}} - \frac{3\alpha_{\text{s}}}{e^2}\left[T_{\text{av}}(x^*,t) - T_{\text{f}}(x^*,0,t)\right]. \tag{6b}$$

The lumped-differential equation (6a) is complemented by the also averaged initial and boundary conditions:

$$T_{\text{av}}(x^*,0) = T_{\infty}(0), \tag{6c}$$

$$-k_{\text{s}} \left.\frac{\partial T_{\text{av}}}{\partial x^*}\right|_{x^*=0} = h_0(t)\left(T_{\infty}(t) - T_{\text{av}}(0,t)\right), \tag{6d}$$

$$k_{\text{s}} \left.\frac{\partial T_{\text{av}}}{\partial x^*}\right|_{x^*=L} = h_L(t)\left(T_{\infty}(t) - T_{\text{av}}(L,t)\right), \tag{6e}$$

where heat losses are also admitted at the two edges of the plate, via prescribed heat transfer coefficients. The conjugated conduction–convection–radiation problem can also be rewritten in dimensionless form after introducing the following variables:

$$U = \frac{u}{u_{\infty}},\ V = \frac{v}{u_{\infty}},\ x = \frac{x^*}{L},\ y = \frac{y^*}{L},\ \tau = \frac{u_{\infty}.t}{L},\ \theta = \frac{T - T_{\infty}(0)}{\frac{\varphi_{\text{ref}}.L}{k_{\text{f}}}},$$

$$\theta_{\infty}(\tau) = \frac{T_{\infty}(t) - T_{\infty}(0)}{\frac{\varphi_{\text{ref}}.L}{k_{\text{f}}}},\ Re_{\text{L}} = \frac{u_{\infty}.L}{\nu},\ Pe_{\text{f}} = \frac{u_{\infty}.L}{\alpha_{\text{f}}},\ Pe_{\text{s}} = \frac{u_{\infty}.e}{\alpha_{\text{s}}},\ \delta_{\text{t}} = \frac{\delta_{\text{t}}^*}{L}, \tag{7}$$

$$Q_{\text{w}} = \frac{\varphi}{\varphi_{\text{ref}}},\ Q_{\text{rad}} = \frac{\varphi_{\text{rad}}}{\varphi_{\text{ref}}},\ R = \frac{e}{L},\ K = \frac{k_{\text{f}}}{k_{\text{s}}},\ Bi_{\text{eff}} = \frac{h_{\text{eff}}.e}{k_{\text{s}}},\ Bi_0 = \frac{h_0.L}{k_{\text{s}}},\ Bi_{\text{L}} = \frac{h_L.L}{k_{\text{s}}}.$$

The flow problem solution is considered known, by any chosen approximate analytical or numerical solution technique. The thermal problem is essentially confined to a region here represented by the steady thickness $\delta_t(x)$, which just needs to be large enough to encompass the actual thermally affected region throughout the transient process. However, it is of interest to avoid the proposition of eigenfunction expansions with variable eigenvalues along the longitudinal coordinate and the time variable. Therefore, we introduce a domain regularization transformation for the spatial domain written as:

$$\eta_{\text{t}} = \frac{y}{\delta_{\text{t}}(x)} \quad \text{and} \quad \chi = x. \tag{8}$$

The dimensionless form for the fluid energy equation after the domain transformation is given by:

$$\delta_t^2(\chi)\frac{\partial\theta_f(\chi,\eta_t,\tau)}{\partial\tau}+\hat{U}\frac{\partial\theta_f(\chi,\eta_t,\tau)}{\partial\chi}+\hat{V}\frac{\partial\theta_f(\chi,\eta_t,\tau)}{\partial\eta_t}=\frac{1}{Pe_L}\frac{\partial^2\theta(\chi,\eta_t,\tau)}{\partial\eta_t^2},$$

$$0<\eta_t<1,\quad 0<\chi<1,\quad \tau>0, \tag{9a}$$

where

$$\hat{U}(\chi,\eta_t)=U(\chi,\eta_t)\delta_t^2(\chi)$$

and

$$\hat{V}(\chi,\eta_t)=\eta_t U(\chi,\eta_t)\delta_t(\chi)\frac{d\delta_t(\chi)}{d\chi}+V(\chi,\eta_t)\delta_t(\chi). \tag{9b}$$

The initial and boundary conditions become:

$$\theta_f(\chi,\eta_t,0)=0,\quad 0<\eta_t<1,\quad 0<\chi\ 1, \tag{9c}$$

$$\theta_f(0,\eta_t,\tau)=\theta_\infty(\tau),\quad 0<\eta_t<1,\quad \tau>0, \tag{9d}$$

$$\theta_f(\chi,1,\tau)=\theta_\infty(\tau),\quad 0<\chi<1,\quad \tau>0, \tag{9e}$$

$$\left.\frac{\partial\theta_f}{\partial\eta_t}\right|_{\eta_t=0}=\delta_t(\chi)\left[Q_{rad}(\chi,\tau)-Q_w(\chi,\tau)\right]$$

$$-\frac{2\delta_t(\chi)\left[3\left(2+Bi_{eff}(\chi,\tau)\right)\theta_{av}(\chi,\tau)-2\left(3+Bi_{eff}(\chi,\tau)\right)\theta_f(\chi,0,\tau)-Bi_{eff}(\chi,\tau)\theta_{¥}(\tau)\right]}{K.R\left(4+Bi_{eff}(\chi,\tau)\right)},$$

$$0<\chi<1,\qquad \tau>0, \tag{9f}$$

where the radiative heat losses at the front face of the plate are computed in a dimensionless form as

$$Q_{rad}(\chi,\tau)=\frac{\varepsilon\sigma}{\varphi_{ref}}\left[\left(T_\infty(0)+\frac{L\varphi_{ref}\theta_f(\chi,0,\tau)}{K.k_s}\right)^4-\left(T_\infty(0)+\frac{L\varphi_{ref}\theta_\infty(\tau)}{K.k_s}\right)^4\right]. \tag{9g}$$

And the wall energy equation with the respective initial and boundary conditions are given by:

$$\frac{\partial \theta_{av}(\chi,\tau)}{\partial \tau} = \frac{R}{Pe_s}\frac{\partial^2 \theta_{av}(\chi,\tau)}{\partial \chi^2}$$

$$+\frac{\left[6\left(2+Bi_{eff}(\chi,\tau)\right)\theta_f(\chi,0,\tau)-12\left(1+Bi_{eff}(\chi,\tau)\right)\theta_{av}(\chi,\tau)-6Bi_{eff}(\chi,\tau)\theta_\infty(\tau)\right]}{Pe_s.R\left(4+Bi_{eff}(\chi,\tau)\right)} \qquad (10a)$$

$$0<\chi<1, \quad \tau>0,$$

$$\theta_{av}(\chi,0)=0, \qquad 0<\chi<1, \qquad (10b)$$

$$\left.\frac{\partial \theta_{av}}{\partial \chi}\right|_{\chi=0} = Bi_0(\tau)\left(\theta_{av}(0,\tau)-\theta_\infty(\tau)\right), \qquad (10c)$$

$$-\left.\frac{\partial \theta_{av}}{\partial \chi}\right|_{\chi=1} = Bi_L(\tau)\left(\theta_{av}(1,\tau)-\theta_\infty(\tau)\right), \quad \tau>0. \qquad (10d)$$

The flow problem is readily solved according to Blasius similarity transformation, which provides the velocity components to feed into the decoupled transient energy equation. For the thermal problem solution, since there is a preferential convective direction aligned with the flow, the integral transformation was chosen to be operated solely in the transversal direction, along which diffusion predominates. However, Eqs. (9) are still not in the most convenient form for integral transformation, since the boundary condition at the interface involves a non-homogeneous term. A filtering solution is then proposed, so as to reduce the importance of the non-homogeneous boundary condition, in the form:

$$\theta_f(\chi,\eta_t,\tau) = \hat{\theta}_f(\chi,\eta_t,\tau) + F(\eta_t;\chi,\tau). \qquad (11)$$

As in [21], a straightforward second degree polynomial filter is proposed, $F(\eta_t; \chi, \tau)$, where χ and τ become parameters of the solution. The filter is obtained from satisfaction of the following three boundary conditions at the transversal domain edges:

$$F(\eta_t,\chi,\tau) = e_0(\chi,\tau) + e_1(\chi,\tau)\eta_t + e_2(\chi,\tau)\eta_t^2, \quad 0<\chi<1, \quad 0<\eta_t<1, \quad \tau>0, \qquad (12a)$$

$$F(1,\chi,\tau) = \theta_\infty(\tau), \qquad (12b)$$

$$\left.\frac{\partial F}{\partial \eta_t}\right|_{\eta_t=1} = 0, \qquad (12c)$$

$$\left.\frac{\partial F}{\partial \eta_t}\right|_{\eta_t=0} = \delta_t(\chi)\left[Q_{\mathrm{rad,F}}(\chi,\tau) - Q_w(\chi,\tau)\right]$$

$$-\frac{2\delta_t(\chi)\left[3\left(2+Bi_{\mathrm{eff}}\right)\theta_{\mathrm{av}}(\chi,\tau) - 2\left(3+Bi_{\mathrm{eff}}\right)F(0,\chi,\tau) - Bi_{\mathrm{eff}}\theta_\infty(\tau)\right]}{K.R\left(4+Bi_{\mathrm{eff}}\right)}, \qquad (12d)$$

$$Q_{\mathrm{rad,F}}(\chi,\tau) = Bi_{\mathrm{rad}}(\tau)\left[F(0,\chi,\tau) - \theta_\infty(\tau)\right],\ h_{\mathrm{rad}} = 4\varepsilon\sigma T_\infty^3(\tau),\ Bi_{\mathrm{rad}} = \frac{h_{\mathrm{rad}}(t)L}{k}, \qquad (12e)$$

where a constant value for a reference Biot number is selected, so as to approximately carry within the filtering solution the information on the effective heat transfer at the back face of the plate. Some information on the radiative losses was also incorporated into the filter, through linearization of the radiative heat transfer at the fluid–solid interface, and with the adoption of a reference radiative heat transfer coefficient. The proposed filter should then be able to provide enough convergence acceleration in the eigenfunction expansions even with the presence of radiative heat exchange at the interface. Thus, applying the proposed filtering solution to Eqs. (9), the resulting filtered problem is given by:

$$\delta_t{}^2(\chi)\frac{\partial\hat{\theta}_f(\chi,\eta_t,\tau)}{\partial\tau} + \hat{U}\frac{\partial\hat{\theta}_f(\chi,\eta_t,\tau)}{\partial\chi} + \hat{V}\frac{\partial\hat{\theta}_f(\chi,\eta_t,\tau)}{\partial\eta_t} = \frac{1}{Pe_f}\frac{\partial^2\hat{\theta}_f(\chi,\eta_t,\tau)}{\partial\eta_t{}^2} + G(\chi,\eta_t,\tau),$$

$$0<\eta_t<1, \qquad 0<\chi<1, \qquad \tau>0, \qquad (13a)$$

where

$$G(\chi,\eta_t,\tau) = -\delta_t{}^2(\chi)\frac{\partial F(\eta_t,\chi,\tau)}{\partial\tau} - \hat{U}\frac{\partial F(\eta_t,\chi,\tau)}{\partial\chi} - \hat{V}\frac{\partial F(\eta_t,\chi,\tau)}{\partial\eta_t} + \frac{1}{Pe_f}\frac{\partial^2 F(\eta_t,\chi,\tau)}{\partial\eta_t{}^2} \qquad (13b)$$

with initial and boundary conditions:

$$\hat{\theta}_f(\chi,\eta_t,0) = -F(\eta_t,\chi,0), \qquad 0<\chi<1, \quad 0<\eta_t<1, \qquad (13c)$$

$$\hat{\theta}_f(0,\eta_t,\tau) = -F(\eta_t,0,\tau), \qquad 0<\eta_t<1, \quad \tau>0, \qquad (13d)$$

$$\left.\frac{\partial\hat{\theta}_f}{\partial\eta_t}\right|_{\eta_t=0} = \left.\frac{\partial\theta_f}{\partial\eta_t}\right|_{\eta_t=0} - \left.\frac{\partial F}{\partial\eta_t}\right|_{\eta_t=0} \qquad (13e)$$

$$\hat{\theta}_f(\chi,1,\tau) = 0, \quad 0<\chi<1, \quad \tau>0. \qquad (13f)$$

The wall energy equation, Eq. (10a), is also modified to incorporate the proposed filtering solution, Eq. (11). Proceeding with application of the Generalized Integral Transform Technique, the proposed auxiliary eigenvalue problem is written as:

$$\frac{d^2\psi(\eta_t)}{d\eta_t^2} + \mu^2\psi(\eta_t) = 0, \qquad 0 < \eta_t < 1, \tag{14a}$$

$$\left.\frac{d\psi}{d\eta_t}\right|_{\eta_t=0} = 0, \tag{14b}$$

$$\psi(1) = 0, \tag{14c}$$

which is readily solved to yield eigenfunctions, eigenvalues, norms, and normalized eigenfuntions, respectively, as:

$$\psi_i(\eta_t) = \mathrm{Cos}\left[\eta_t\mu_i\right], \qquad 0 < \eta_t < 1, \qquad i = 1,2,\ldots, \tag{15a}$$

$$\mu_i = \frac{(2i-1)\pi}{2}, \quad i = 1,2,\ldots, \tag{15b}$$

$$N_i = \int_0^1 \psi_i(\eta_t)\psi_i(\eta_t)d\eta_t = 1/2, \tag{15c}$$

$$\tilde{\psi}_i(\eta_t) = \frac{\tilde{\psi}_i(\eta_t)}{N_i^{1/2}} = \sqrt{2}\mathrm{Cos}\left[\eta_t\mu_i\right], \qquad 0 < \eta_t < 1, \qquad i = 1,2,\ldots . \tag{15d}$$

The eigenvalue problem (14) allows definition of the following transform–inverse pair:

$$\bar{\hat{\theta}}_{f,j}(\chi,\tau) = \int_0^1 \tilde{\psi}_j(\eta_t)\hat{\theta}_f(\chi,\eta_t,\tau)\,d\eta_t \qquad \rightarrow \quad \text{Transform}, \tag{16a}$$

$$\hat{\theta}_f(\chi,\eta_t,\tau) = \sum_{j=1}^{\infty} \tilde{\psi}_j(\eta_t)\bar{\hat{\theta}}_{f,j}(\chi,\tau) \qquad \rightarrow \quad \text{Inverse}. \tag{16b}$$

Applying the operator $\int_0^1 \tilde{\psi}_i(\eta_t)d\eta_t$ over Eq. (13a), followed by the inverse formula, then results:

$$\delta_t^{\,2}(\chi)\frac{\partial\bar{\hat{\theta}}_{f,i}(\chi,\tau)}{\partial\tau}+\sum_{j=1}^{\infty}\left[a_{ij}(\chi)\frac{\partial\bar{\hat{\theta}}_{f,j}(\chi,\tau)}{\partial\chi}+b_{ij}(\chi)\bar{\hat{\theta}}_{f,j}(\chi,\tau)\right]+c_i(\chi,\tau)=\bar{g}_i(\chi,\tau), \qquad (17a)$$

$$0<\chi<1, \qquad \tau>0, \qquad i=1,2,\ldots,$$

$$\bar{\hat{\theta}}_{f,i}(\chi,0)=-\int_0^1\tilde{\psi}_i(\eta_t)F(\eta_t,\chi,0)\,d\eta_t, \qquad (17b)$$

$$\bar{\hat{\theta}}_{f,i}(0,\tau)=-\int_0^1\tilde{\psi}_i(\eta_t)F(\eta_t,0,\tau)\,d\eta_t, \qquad (17c)$$

$$a_{ij}(\chi)=\int_0^1\hat{U}(\chi,\eta_t)\,\tilde{\psi}_i(\eta_t)\tilde{\psi}_j(\eta_t)d\eta_t=\delta_t^{\,2}(\chi)\int_0^1U(\eta_t)\,\tilde{\psi}_i(\eta_t)\tilde{\psi}_j(\eta_t)d\eta_t, \qquad (17d)$$

$$b_{ij}(\chi)=\frac{1}{Pe_f}\mu_j^{\,2}\delta_{ij}+\int_0^1\hat{V}(\chi,\eta_t)\,\tilde{\psi}_i(\eta_t)\frac{d\tilde{\psi}_j(\eta_t)}{d\eta_t}d\eta_t, \qquad (17e)$$

$$c_i(\chi,\tau)=\frac{1}{Pe_f}\tilde{\psi}_i(0)\left.\frac{\partial\hat{\theta}_f}{\partial\eta_t}\right|_{\eta_t=0}=\sqrt{2}\,\frac{1}{Pe_f}\left(\left.\frac{\partial\theta_f}{\partial\eta_t}\right|_{\eta_t=0}-\left.\frac{\partial F}{\partial\eta_t}\right|_{\eta_t=0}\right), \qquad (17f)$$

$$c_i(\chi,\tau)=\sqrt{2}\,\frac{\delta_t(\chi)}{Pe_f}\left\{\left(\frac{2\left[3\left(2+Bi_{eff}\right)\theta_{av}(\chi,\tau)-2\left(3+Bi_{eff}\right)F(0,\chi,\tau)-Bi_{eff}\,\theta_\infty(\tau)\right]}{K.R\left(4+Bi_{eff}\right)}\right)\right.$$

$$-\left(\frac{2\left[3\left(2+Bi_{eff}\right)\theta_{av}(\chi,\tau)-2\left(3+Bi_{eff}\right)\theta_f(\chi,0,\tau)-Bi_{eff}\,\theta_\infty(\tau)\right]}{K.R\left(4+Bi_{eff}\right)}\right)$$

$$\left.+\left[Q_{rad}(\chi,\tau)-Q_{rad,F}(\chi,\tau)\right]\right\}, \qquad (17g)$$

$$Q_{\mathrm{rad}}(\chi,\tau)=\frac{\varepsilon\sigma}{\varphi_{\mathrm{ref}}}\left[T_{\infty}(0)+\frac{L\varphi_{\mathrm{ref}}}{k_{\mathrm{f}}}\left(F(\chi,0,\tau)+\sqrt{2}\sum_{j=1}^{\infty}\bar{\hat{\theta}}_{\mathrm{f,j}}(\tau)\right)\right]^4$$

$$-\frac{\varepsilon\sigma}{\varphi_{\mathrm{ref}}}\left[T_{\infty}(0)+\frac{L\varphi_{\mathrm{ref}}\theta_{\infty}(\tau)}{k_{\mathrm{f}}}\right]^4, \tag{17h}$$

$$\overline{g_{\mathrm{i}}}(\chi)=-\int_0^1\tilde{\psi}_{\mathrm{i}}(\eta_{\mathrm{t}})\delta_{\mathrm{t}}{}^2(\chi)\frac{\partial F(\eta_{\mathrm{t}},\chi,\tau)}{\partial\tau}d\eta_{\mathrm{t}}-\int_0^1\tilde{\psi}_{\mathrm{i}}(\eta_{\mathrm{t}})\hat{U}\frac{\partial F(\eta_{\mathrm{t}},\chi,\tau)}{\partial\chi}d\eta_{\mathrm{t}}$$

$$-\int_0^1\tilde{\psi}_{\mathrm{i}}(\eta_{\mathrm{t}})\hat{V}\frac{\partial F(\eta_{\mathrm{t}},\chi,\tau)}{\partial\eta_{\mathrm{t}}}d\eta_{\mathrm{t}}+\int_0^1\tilde{\psi}_{\mathrm{i}}(\eta_{\mathrm{t}})\frac{1}{Pe_{\mathrm{f}}}\frac{\partial^2F(\eta_{\mathrm{t}},\chi,\tau)}{\partial\eta_{\mathrm{t}}{}^2}d\eta_{\mathrm{t}}. \tag{17i}$$

The wall heat transfer problem can then be described by the partial differential equation (10a) coupled to the transformed fluid temperature fields. Equations (17) and (10) form an infinite coupled system of one-dimensional partial differential equations for the fluid transformed potentials and the wall average temperature. For computational purposes this system is truncated to a sufficiently large finite order, N, for the required convergence control. The PDE system is then numerically handled by routine NDSolve of the *Mathematica* v.7.0 system [23]. Once the transformed potentials are numerically computed, the inversion formula, Eq. (16b), is employed to reconstruct the filtered potentials, in explicit form in the transversal coordinate, and after adding the filtering solution, $F(\eta_t; \chi, \tau)$, the dimensionless temperature distribution, $\theta_t(\chi, \eta_t, \tau)$, is recovered everywhere within the boundary layer and along the transient process.

3. EXPERIMENTAL APPARATUS

An experimental setup was assembled for the measurement by an infrared camera of both temporal and spatial evolutions of the temperature on the front surface of a 330 × 250 mm^2 black PVC plate (Fig. 1). The plate (1) was heated by two flash lamps (8) that have been placed normally to its front face, controlled by an electronic timer (9). The plate is maintained vertically at the outlet of a rectangular channel, with 300 × 250 cross flow section (2). The plate contains dissipative fluxmeters, for the incident heat flux measurements. The airflow, generated by a double aspiration fan (3), was directed via a flow calming section in the channel with 700 mm in straight length. This channel allows the airflow to be parallel to the plate and covering the entire of its width. An AC converter voltage (4) controls the fan. The flow velocity associated with each voltage used in the tests was preliminarily measured by a propeller anemometer on the outlet section of the channel.

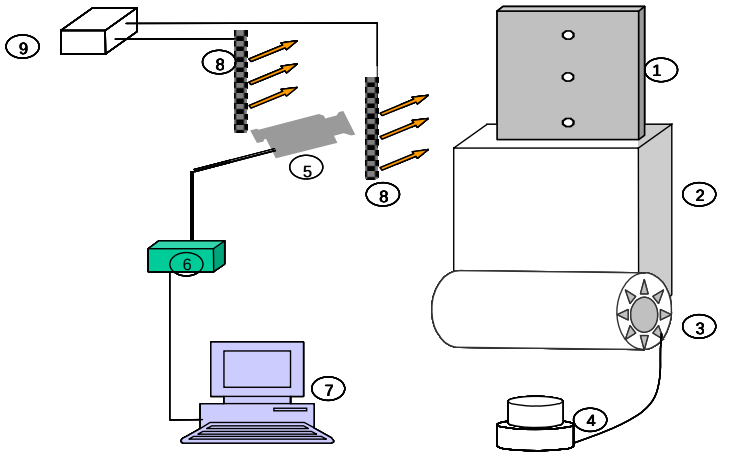

Fig. 1. Experimental setup for conjugated convection–conduction–radiation analysis.

Cartographies of temperature distribution have been obtained by a short-wave infrared camera (5), installed as shown in Fig. 2. For recording the infrared frames, the camera was connected to the digital interface box (6). A cable connects the interface box to a breakout box, from which a second cable is connected to the PCMCIA card interface mounted on a computer station (7). The proprietary software allows recording infrared images with 50 Hz sample rate.

The thermophysical properties of the black PVC were measured on the Netzsch Nanoflash LFA 447/1 available in the Laboratory of Heat Transmission and Technology (LTTC/COPPE/UFRJ). The LFA 447/1 is a tabletop instrument that works with a high power Xenon-Flash lamp in the temperature range of room temperature to 200^{o}C, and it has an integrated sample changer for 4 samples. The LFA 447/1 is ca-

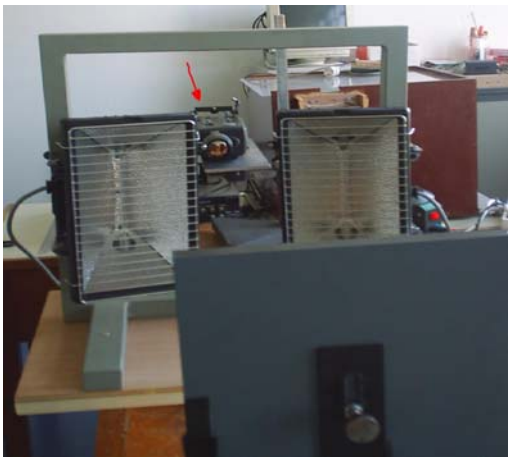

Fig. 2. Detail of the flash lamps and the infrared camera as viewed from behind the heated plate.

pable of measuring thermal diffusivity in the range of 0.01 mm^2/s up to 1000 mm^2/s, with an accuracy of 3–5% for most materials. The specific heat accuracy is 5–7%. This allows the calculation of the thermal conductivity in the range of 0.1 to 2000 W/m·K with an accuracy of 3–7% for most materials [24]. The analysis of experimental data was performed with a software called Proteus, provided by Netzsch, providing the following thermophysical properties estimates at 25°C: α = 0.144 mm^2/s, k = 0.164 W/m·°C, and c_p = 798 J/kg·°C.

4. RESULTS AND DISCUSSION

The experimental configuration considered in the present analysis adopts a black PVC plate of 33 cm in height, thickness of 12 mm, and 20 cm wide. The configuration was aimed at insulating the PVC plate within a Styrofoam assembly of 8 cm in thickness at the back face and 3.8 cm at the lateral faces. The flash lamps are maintained continuously heating the plate at the same power level.

Thermograms were constructed for the transient evolution of the front face temperatures, such as shown in Fig. 3, here for the case of an imposed interface heat flux of ϕ = 541.5 W/m^2 starting at t = 0. Also, temperature measurements at the back face of the plate and insulating material were registered to allow estimation of the heat losses. For this situation of an insulated plate, an effective heat transfer coefficient representing the heat losses through the insulating material to the surroundings on the back face was estimated as a function of time and position, from the

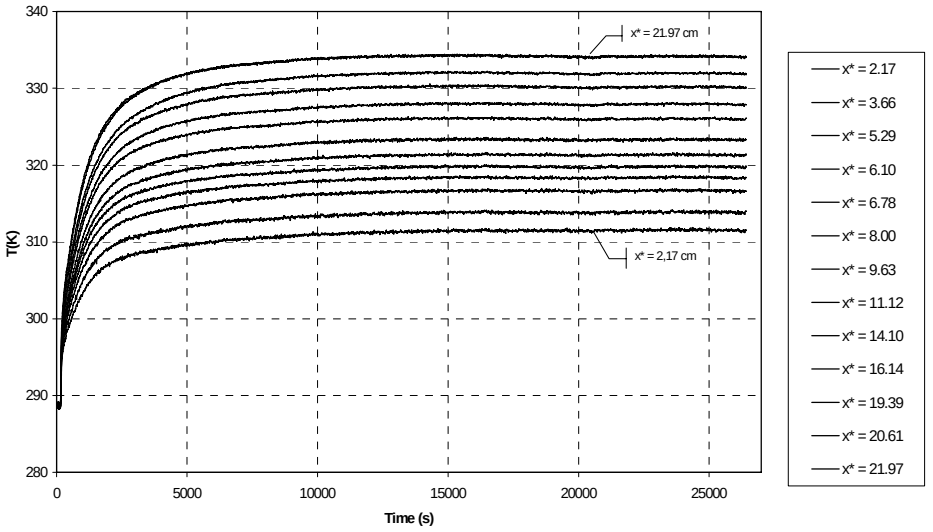

Fig. 3. Thermograms of acquired temperature evolutions with infrared camera (black PVC plate, e = 12 mm, ϕ = 541.5 W/m^2, u_∞ = 2.2 m/s, insulated back and lateral faces).

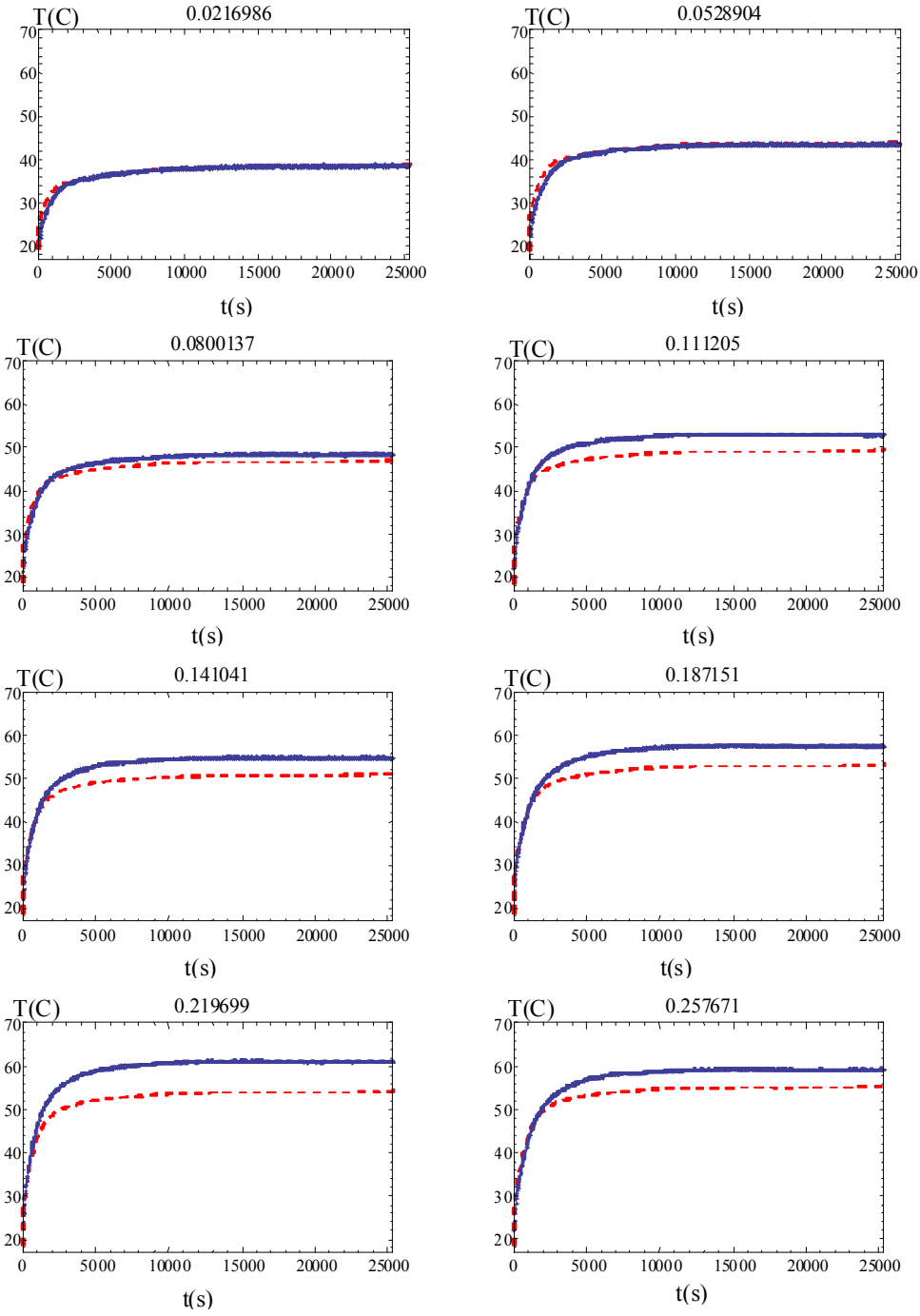
T(C)
0.0216986
T(C)
0.0528904
T(C)
0.0800137
T(C)
0.111205
T(C)
0.141041
T(C)
0.187151
T(C)
0.219699
T(C)
0.257671
t(s)

Fig

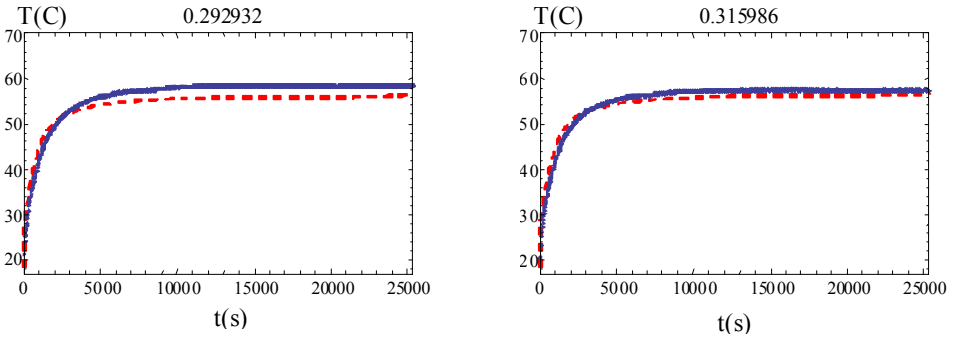

Fig. 4. Comparison of transient behavior of front face temperatures along the plate length (x = 2.17, 5.29, 8.00, 11.1, 14.1, 18.7, 22.0, 25.8, 29.3, and 31.6 cm), theoretical (dashed lines) and experimental (solid lines).

available temperature measurements and correlations for natural convection, also accounting for the radiative losses from the insulation. A typical average value for this effective coefficient along most of the transient was around 4.5 W/m$^{2.o}$C. At the trailing and leading edges the estimated value is given by $h_L = h_0$ =1.6 W/m$^{2.o}$C. It has been noticed that the free stream temperature is fairly variable along the heating process, and thus it was considered as a function of time in the model, after being interpolated into a continuous function.

Therefore, Figs. 4 present a comparison of the experimental (solid curves) and theoretical results (dashed curves) for the temperature evolutions at the plate front face, for selected positions x distributed along the plate length. In general, the set of results for the hybrid simulation presents a fairly reasonable agreement against the experimental results, with improved adherence for smaller x positions along the plate (up to around 1/3 of the plate length) and, less markedly, at the earlier transient. Figures 4 also show that there exists significant flow recirculation around the leading edge of the plate, due to the positioning of the plate within the air stream, and that some improvement on this flow arrangement is required for a more adequate comparison of the heat transfer results from the present boundary layer modeling, for regions close to the plate leading edge. Such results in part explain the lower temperature values attained by the boundary layer theoretical analysis for the very lower values of the longitudinal position x.

On the other hand, Figs. 5a,b show the behavior of the thermography measurements both as a function of time at selected positions, Fig. 5a, as well as along the plate length, for a few selected time values, Fig. 5b. It can be clearly observed that although the time behavior of the temperature values indicated by the camera have the expected trends for this physical problem, the spatial behavior presents a number of peaks that are not associated with the physical behavior for the present problem (for instance, at x around 13, 17, and 21 cm, as pointed out in Fig. 5b), but rather to a probable space variation of the surface emissivity. The vicinities of these peaks

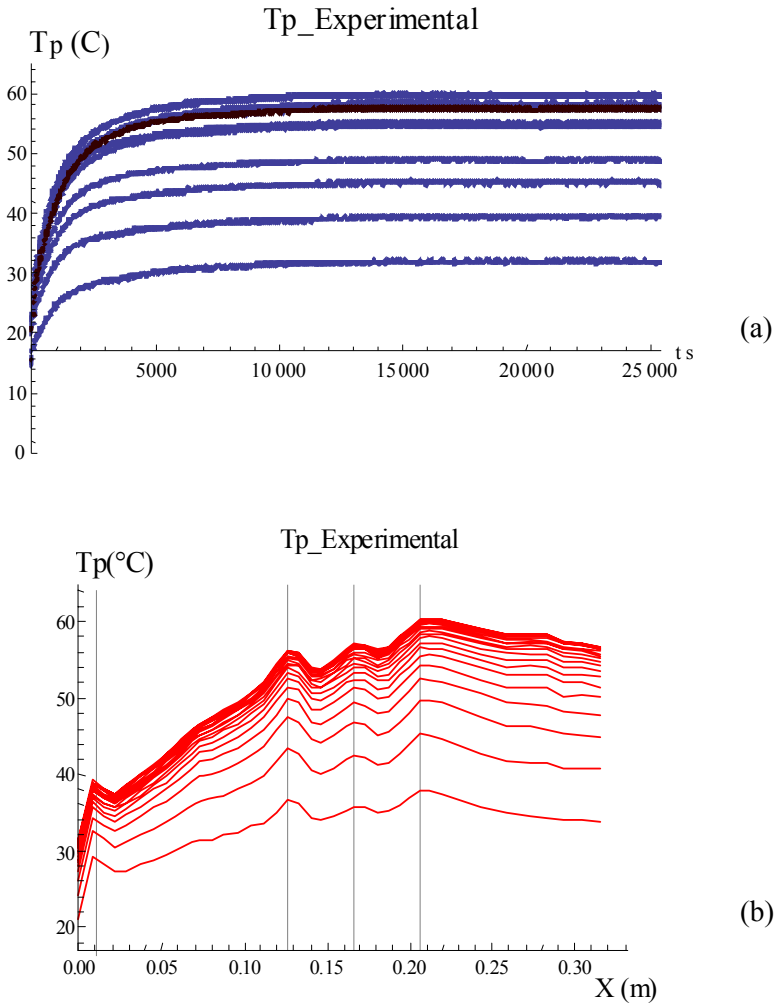

Fig. 5. (a) Transient behavior of measured temperatures at various positions along the plate length; (b) Spatial variation of measured temperatures at various time values.

indicate the regions of more noticeable deviation between the measured and simulated results, and as expected from Fig. 5b, with the measured value always above the theoretical result. Since the camera software transforms the information of digital level into absolute temperatures by taking the user provided reference uniform emissivity, reference temperature measurements and the corresponding emissivity at that point are necessary to reprocess the information provided by the software, which was not available in the present experimental run, and then adjust the measured temperatures. Thus, in the present simulations, a plain uniform emissivity of 0.93 was assumed at the plate front face, typical of flat black oil paint (www.infrared-thermography.com).

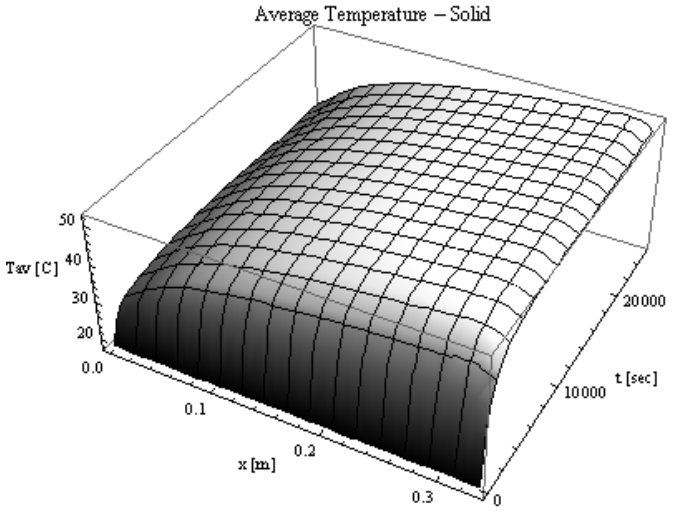

(a)

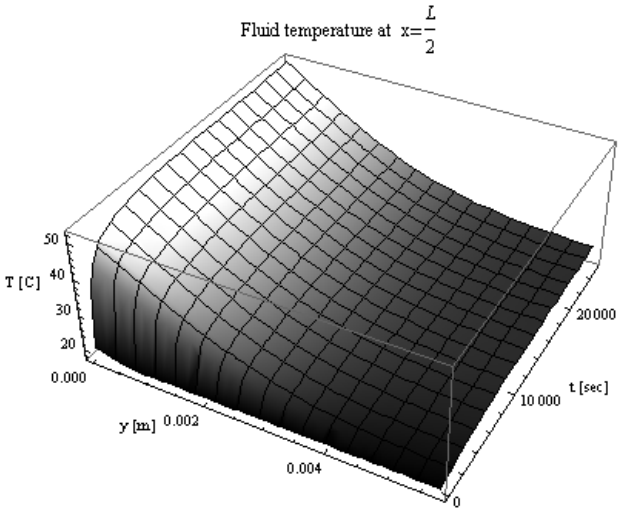

(b)

Fig. 6. (a) Spatial and temporal variation of the simulated average solid wall temperature; (b) Spatial (transversal) and temporal variation of the simulated fluid temperature at half the length of the plate ($x = L/2$).

Figures 6a,b illustrate the simulation for the transient behavior of both the average solid temperature, along the plate length, and the fluid temperature across the transversal coordinate, at half the length of the plate ($x = L/2$). One may clearly observe the coupled transient behavior of the two fields, the thermal boundary layer development within the fluid as one approaches the interface, and the increased heating of the plate as the effective heat transfer coefficient progressively reduces along the plate length. The smoothness of the simulated temperature evolutions both in time and space, serve to reconfirm that the spatial variation in the measured temperatures

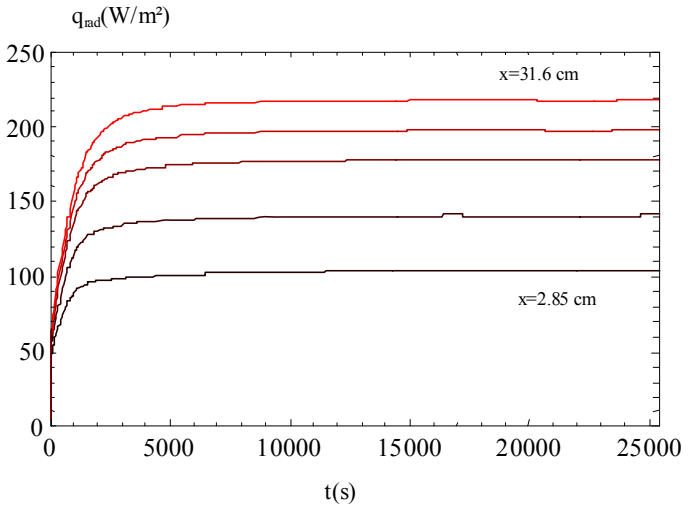

Fig. 7. Transient behavior of front face radiative heat fluxes along the plate length (x = 2.85, 6.78, 14.1, 20.6, and 31.6 cm), from the lower curve (x = 2.85 cm) to the upper curve (x = 31.6 cm).

are not pertinent to the modeled heat transfer phenomena, but due to measurement discrepancies in light of surface conditions variability.

Finally, from Fig. 7 for the evolution of the radiation heat flux at the plate front face, at selected positions x = 2.85, 6.78, 14.1, 20.6, and 31.6 cm, one may clearly notice the major importance of radiative losses from the illuminated plate face, reaching values around 220 W/m^2 at the higher positions and large times, which once neglected would introduce significant errors in the prediction of the present heat transfer problem behavior. Thus, the proposed model provides the important conclusion that radiation heat transfer cannot be possibly neglected from this conjugated problem, in light of the achievable radiative heat fluxes of the same order of magnitude as the applied and convective heat fluxes.

ACKNOWLEDGMENTS

The authors (CPN and RMC) would like to acknowledge the kind hospitality of the Laboratoire de Thermomécanique, Université de Reims, France, during their stay in January–February 2008, and would like to acknowledge the financial support provided by ICHMT and CNPq/Brasil.

NOMENCLATURE

$h(x, t)$	heat transfer coefficient at the interface, W/m^2.^{o}C
k_f	thermal conductivity (fluid), W·m^{-1}·K^{-1}

k_s thermal conductivity (solid), $W \cdot m^{-1} \cdot K^{-1}$
L plate length, m
Pe Peclet number
Q_w dimensionless imposed interface heat flux
Q_{rad} dimensionless radiative heat flux at the front face
Re_L Reynolds number
t time variable, s
T_∞ free stream temperature, ^oC
T_f fluid temperature, ^oC
T_s solid temperature, ^oC
T_{av} averaged wall temperature, ^oC
u_∞ free stream velocity, $m \cdot s^{-1}$
u longitudinal velocity component, $m \cdot s^{-1}$
U dimensionless longitudinal velocity component
v transversal velocity component, $m \cdot s^{-1}$
V dimensionless transversal velocity component
x^* longitudinal coordinate, m
x dimensionless longitudinal coordinate
y^* transversal coordinate, m
y dimensionless transversal coordinate

Greek symbols

α_f thermal diffusivity (fluid), $m^2 \cdot s^{-1}$
α_s thermal diffusivity (solid), $m^2 \cdot s^{-1}$
χ dimensionless transformed longitudinal coordinate
η_t dimensionless transformed transversal coordinate
$\delta^*(x)$ velocity boundary-layer thickness, m
$\delta(\chi)$ dimensionless velocity boundary-layer thickness
$\delta_t^*(x)$ thermal boundary-layer thickness, m
$\delta_t(\chi)$ dimensionless thermal boundary-layer thickness
θ_f dimensionless temperature (fluid)
θ_{av} dimensionless averaged wall temperature (solid)
ν kinematic viscosity, $m^2 \cdot s^{-1}$
τ dimensionless time
$\phi(x^*, t)$ imposed interface heat flux, W/m^2
ϕ_{ref} reference heat flux at the interface, W/m^2.

REFERENCES

1. Perelman, T. L. On conjugate problems of heat transfer, *Int. J. Heat Mass Transfer*, Vol. 3, pp. 293–303, 1961.
2. Luikov, A. V., Aleksashenko, V. A., and Aleksashenko, A. A. Analytical methods of solution of conjugated problems in convective heat transfer, *Int. J. Heat Mass Transfer*, Vol. 14, pp. 1047–1056, 1971.

3. Guedes, R. O. C., Cotta, R. M., and Brum, N. C. L. Heat transfer in laminar tube flow with wall axial conduction effects, *J. Thermophys. Heat Transfer*, Vol. 5, No. 4, pp. 508–513, 1991.
4. Vynnycky, M., Kimura, S., Kanev, K., and Pop, I. Forced convection heat transfer from a flat plate: the conjugate problem, *Int. J. Heat Mass Transfer*, Vol. 41, pp. 45–59, 1998.
5. Mossad, M. Laminar forced convection conjugate heat transfer over a flat plate, *Heat Mass Transfer*, Vol. 35, pp. 371–375, 1999.
6. Pozzi, A. and Tognaccini, R. Coupling of conduction and convection past an impulsively started semi-infinite flat plate, *Int. J. Heat Mass Transfer*, Vol. 43, pp. 1121–1131, 2000.
7. Lachi, M., Rebay, M., Mladin, E., and Padet, J. Integral approach of the transient coupled heat transfer over a plate exposed to a variation in the input heat flux, *ICHMT Int. Symp. Transient Convective Heat and Mass Transfer in Single & Two-Phase Flows*, August, Cesme, Turkey, 2003.
8. Cotta, R. M. *Integral Transforms in Computational Heat and Fluid Flow*, CRC Press, Boca Raton, Florida, USA, 1993.
9. Cotta, R. M. and Mikhailov, M. D. *Heat Conduction: Lumped Analysis, Integral Transforms, Symbolic Computation*, Wiley-Interscience, New York, 1997.
10. Cotta, R. M. (Ed.) *The Integral Transform Method in Thermal and Fluids Sciences and Engineering*, Begell House, New York, USA, 1998.
11. Santos, C. A. C., Quaresma, J. N. N., and Lima, J. A. *Benchmark Results for Convective Heat Transfer in Ducts: — The Integral Transform Approach*, ABCM Mechanical Sciences Series, Ed. E-Papers, Rio de Janeiro, 2001.
12. Cotta, R. M. and Mikhailov, M. D. Hybrid Methods and Symbolic Computations, in: W. J. Minkowycz, E. M. Sparrow, and J. Y. Murthy (Eds.), *Handbook of Numerical Heat Transfer*, 2nd ed., Ch. 16, John Wiley, New York, pp. 493–522, 2006.
13. Cotta, R. M., Mikhailov, M. D., and Ozisik, M. N. Transient conjugated forced convection in ducts with periodically varying inlet temperature, *Int J. Heat Mass Transfer*, Vol. 30, No. 10, pp. 2073–2082, 1987.
14. Guedes, R. O. C. and Cotta, R. M. Periodic laminar forced convection within ducts including wall heat conduction effects, *Int. J. Eng. Sci*., Vol. 29, No. 5, pp. 535–547, 1991.
15. Guedes, R. O. C., Cotta, R. M., and Özisik, M. N. Conjugated periodic turbulent forced convection in a parallel plate channel, *J. Heat Transfer*, Vol. 116, pp. 40–46, 1994.
16. Lachi, M., Cotta, R. M., Naveira, C. P., and Padet, J. Improved lumped-differential formulation of transient conjugated conduction-convection in external flow, in: *Proc. 11th Brazilian Congress of Thermal Sciences and Engineering*, ENCIT 2006, Curitiba, Brasil, Paper no. CIT06-0965, December 2006.

17. Remy, M., Degiovanni, A., and Maillet, D. Mesure de Coefficient d'Échange pour des Écoulements à Faible Vitesse, Rev. Gén. Therm., Vol. 397, pp. 28–42, 1995.
18. Rebay, M., Lachi, M., and Padet, J. Mesure de coefficients de convection par méthode impulsionnelle–influence de la perturbation de la couche limite, *Int. J. Thermal Sci*., Vol. 41, pp. 1161–1175, 2002.
19. Rebay, M., Mladin, E., Chemin, S., and Stoian, M. Dissipative fluxmeter for the validation of the heat transfer coefficient measurement by the pulsed method, *Eurotherm 2008*, Eindhoven, Netherlands, June 2008.
20. Naveira, C. P., Cotta, R. M., Lachi, M., and Padet, J. Transient Conjugated Conduction-External Convection with Front Face Imposed Wall Heat Flux, in: *Proc. IMECE2007, ASME International Mechanical Engineering Congress & Exposition*, Paper no. IMECE2007-41417, Seattle, Washington, USA, November 11–15, 2007.
21. Naveira, C. P., Lachi, M., Cotta, R. M., and Padet, J. Hybrid Formulation and Solution for Transient Conjugated Conduction-External Convection, *Int. J. Heat Mass Transfer*, Vol. 52, Nos. 1–2, pp. 112–123, 2009.
22. Aparecido, J. B. and Cotta, R. M. Improved One-Dimensional Fin Solutions, *Heat Transfer Eng*., Vol. 11, No. 1, pp. 49–59, 1989.
23. Wolfram, S. *The Mathematica Book*, version 7.0, Cambridge-Wolfram Media, 2008.
24. Pinto, C. S. C., Massard, H., Couto, P., Orlande, H. R. B., Cotta, R. M., and Ambrosio, M. C. R. Measurement of thermophysical properties of ceramics by the flash method, *METROSUL IV, 4th Congresso Latino-Americano de Metrologia*, Foz do Iguaçú, November 2004; also, *Brazilian Archives of Biology and Technology*, Vol. 48, pp. 31–39, 2006.

□◆◆◆□